



# Improving the machining performance with bio-degradable coconut oil-assisted MQL turning of AISI-1040 steel: a sustainable machining approach

Saurabh Tiwari<sup>1</sup> · M Amarnath<sup>1</sup>

Received: 10 April 2023 / Revised: 15 June 2023 / Accepted: 29 June 2023  
© The Author(s), under exclusive licence to Springer-Verlag GmbH Germany, part of Springer Nature 2023

## Abstract

To counteract the adverse effects of mineral oil-based cutting fluids, manufacturing industries are aspire toward environment-friendly and less toxic cutting fluids. The biodegradability and non-toxic characteristics of vegetable oils make them an appropriate alternative to mineral oil-based cutting fluids. In this context, this research article presents the results of an experimental investigation carried out to improve the machining performance of AISI-1040 steel by utilizing coconut oil (CO) as a cutting fluid with minimum quantity lubrication and cooling (MQL) technique. A detailed investigation and analysis of tool flank wear, crater wear, cutting tool vibration, surface topography, cutting zone temperature, and chip morphology were performed under dry, flood, mineral oil with MQL (MQL-MO), and coconut oil with MQL (MQL-CO) cutting conditions. The findings of this investigation revealed that the MQL-CO is highly efficient in minimizing friction and heat dissipation. The tool wear was reduced by 52–58%, 33–37%, and 14–17% under MQL-CO as compared to dry, flood, and MQL-MO cutting conditions. In addition, the surface roughness values were reduced by 48%, 24%, and 22% and the cutting temperature was reduced by 40%, 22%, and 13% under MQL-CO than that of dry, flood, and MQL-MO cutting conditions. The MQL-CO cutting condition showed a considerable reduction in cutting tool vibration acceleration levels and a favorable chip morphology which improved the machining performance.

**Keywords** Minimum quantity lubrication · Sustainable manufacturing · Crater wear depth · IR thermography · tool vibration

## Nomenclature

MQL	Minimum quantity lubrication
CO	Coconut oil
MO	Mineral oil
AISI	American Iron and Steel Institute
IR	Infrared
$\theta_w$	Wetting angle
$R_a$	Average surface roughness
$V_B$	Flank wear
$K_T$	Crater wear depth
$Q_{c-t}$	Heat generated at chip-tool interface

$Q_{w-t}$	Heat generated at workpiece-tool interface
$v_c$	Cutting speed
$f$	Feed rate
$a_p$	Depth of cut

## 1 Introduction

In the machining process, shearing action of cutting tool on work material causes metal to deform plastically which generates a large amount of heat. This heat resulted in a high temperature at the tool-workpiece interaction zone. As a consequence, faster tool wear occurs that directly affects the tool life, surface finish quality, power consumption, and dimensional accuracy [1]. To dissipate this heat, mineral-oil-based cutting fluids are extensively used as a coolant. However, these fluids are non-biodegradable and highly toxic in nature which leads to harmful effects on operators' health and the environmental ecosystem. The vaporization and direct contact of these fluids may cause respiratory and

✉ Saurabh Tiwari  
saurabhgtiwari@gmail.com

✉ M Amarnath  
amarnath.cmy@gmail.com

<sup>1</sup> Tribology and Machine Dynamics Laboratory, Department of Mechanical Engineering, Indian Institute of Information Technology, Design, and Manufacturing, Jabalpur, Madhya Pradesh 482005, India

skin-related health issues such as chronic bronchitis, asthma, airway irritation, folliculitis, etc. Furthermore, these fluids possess organic compounds which persist for a longer duration in water and soil, resulting in higher disposal costs and ultimately higher production costs [2–5]. Hence, the utilization of mineral oils as a cutting fluid resulted in a slew of environmental, financial, and health difficulties. In consequence, the researchers are forced to pay attention to the innovation of environment-friendly and less toxic cutting fluids to make a step towards sustainable manufacturing. Sustainability involves economic, environmental, and social aspects of the manufacturing process. The primary goal of sustainability is to manufacture the desired product at a low cost by reducing the negative impact on the ecosystem and human health with minimum wastage of energy and natural resources [6–8].

From the perspective of the aforementioned challenges, the various attributes of vegetable oils such as biodegradability, high viscosity index, low volatility, and good lubricity make them a suitable alternative to mineral oil-based cutting fluids. In addition, vegetable oils consist of higher boiling point temperatures and larger molecular weight characteristics which significantly reduces vaporization. The molecular arrangement of vegetable oil consists of a long chain molecule of saturated and unsaturated fatty acids. In saturated fatty acids, the chain does not contain a double bond, hence the molecules can effectively arrange themselves in a straight chain that is densely packed on metal contact surfaces. This forms a protective layer on the sliding contact surfaces thereby causing a reduction in friction and wear [9–11]. On the other hand, effectiveness of the cutting fluids also depends on the technique of application. In the conventional flood pouring technique, coolant is unable to penetrate the cutting zone as a result the intended cooling performance is not achieved. However, the cooling/lubricating performance can be improved by utilizing minimum quantity lubrication and cooling (MQL) technique. In MQL, a minute quantity of cutting fluid is sprayed into the cutting zone in the form of a pressurized aerosol mist with the help of a nozzle. The aerosol mist is created by the atomization process in which the pressurized air from the compressor is allowed to mix with the cooling media which intern converts the liquid into a group of tiny droplets. These tiny droplets impinge directly on the interacting surfaces to provide cooling and lubrication. The MQL considerably reduces the consumption of coolant and has proven to be a more economical and environment-friendly technique [12].

Numerous experimental investigations have presented the significance of vegetable oils with MQL in various machining processes such as drilling, turning, milling, grinding, etc. [13]. Sen et al. [14] investigated the cooling and lubricating performance of palm oil during the milling operation of Inconel 690 steel. The experiments were carried out by

using mineral-based oil with flood pouring and palm oil with MQL technique. The authors highlighted that the palm oil with MQL resulted in a better surface finish and lesser tool wear than the mineral-based oil. Revuru et al. [15] examined the performance of soyabean oil as a cutting fluid with MQL while turning 4140 steel. The dry, flood with mineral-based oil, and palm oil with MQL was considered as cutting conditions during the experiments with various cutting speeds and feed rates while the depth of cut remained constant. The study concluded that palm oil with the MQL showed a considerable reduction in surface roughness, tool wear, and cutting zone temperature compared to other cutting conditions. Özbek and Saruhan [16] carried out an experimental investigation on the performance evaluation of vegetable-based SAMNOS ZM-22W as a cutting fluid under MQL while turning AISI D2 steel. The tool vibration, cutting temperature, tool wear, and surface roughness were utilized as a performance indicator and the results are compared with dry cutting conditions. The authors concluded that considerable reduction in tool vibration, cutting temperature, and tool wear with better surface finish quality were observed under vegetable-based cutting fluid in comparison with dry cutting condition. Krishna et al. [17] experimentally investigated the cooling performance of water-soluble oil (SAE-40) and coconut oil during the turning of AISI 1040 steel. Both the coolants were supplied with a gravity-feed lubrication setup. Their results showed a considerable decrease in cutting zone temperature, flank wear, and surface waviness with coconut oil as a cutting fluid in comparison with water-soluble oil. Wang et al. [18] presented a review on the sustainability of vegetable oil-based cutting fluids in turning operation. The authors have discussed the effect of physical and chemical properties of vegetable oils in the machining process. Their review summarizes that the viscosity, fatty acid composition, and carbon chain length are the key factors to enhance the cooling and lubricating performance of vegetable oils. Liu et al. [19] proposed a surface roughness prediction model during the milling operation. The influence of stepover ratio, minor cutting-edge angle, corner radius, and feed per tooth on surface roughness was analysed through numerical simulation. The milling operation was carried out to verify the proposed surface prediction model and compared it with surface 3D topography based on the Z-map prediction model. The authors have concluded that the average width of the surface profile ( $R_{sm}$ ) and average height deviation of surface profile ( $R_a$ ) parameters were accurately predicted with the proposed model.

The tool-workpiece-chip interaction at the cutting region generates a high cutting temperature during the machining process which directly influences the surface integrity, geometric accuracy, and most importantly the tool wear/life [20]. Thus, the assessment of cutting temperature is of vital importance during the turning operation. Several

experimental investigations showed the reliability of infrared (IR) thermography to measure the cutting zone temperature. Paramasivam [21] utilized the IR thermography technique to evaluate the cutting zone temperature during the boring operation. The investigation showed that IR thermography can measure the tool temperature with higher accuracy. Further, the tool temperature will be increased with the increase in tool wear. Arrazola et al. [22] employed IR thermography to determine the tool side face and tool chip contact temperature during the metal cutting operation. The study showed that IR thermography can be used to measure the cutting temperature with a high degree of accuracy. They also revealed that the tool-chip contact region showed a maximum temperature than that of the tool side face. Prasad et al. [23] proposed a tool condition monitoring technique based on tool vibration and cutting temperature analysis to evaluate the tool wear while turning AISI 316L steel. A laser Doppler vibrometer was used to acquire the vibratory signals and a FLIR IR thermal camera is used to record the cutting temperature. The results concluded that as the tool wear progresses, the amplitude of vibration signals and cutting temperature increased uniformly.

On the other hand, rotation of the workpiece along with the action of cutting tool results in vibration during the machining process. It is one of the important considerations in machining which influences tool wear and cutting zone temperature. The cutting process interruptions, tool wear, and other machining-related disturbance are the immediate results of vibration, which indeed reduces the surface quality and thereby minimizes the cutting tool life [24, 25]. Several studies had been carried out to measure the tool vibrations by using various types of sensors. Orhan et al. [26] conducted an experimental study to detect tool wear during turning operation by using vibration monitoring techniques. The authors concluded that the increase in tool wear can be correlated to the increase in rms values of the cutting tool vibration signals. Rmili et al. [27] proposed an automatic tool wear monitoring system based on mean power analysis of the vibration signals. A tri-axial piezo-electric accelerometer was used to acquire the vibration signal of the tool holder during the turning operation and an optical microscope was used to measure the flank wear. The three conventional phases of tool life, viz., tool breaking-in, stabilization, and acceleration of wear, were distinguished from vibration signal response based on mean power analysis. The authors concluded that the mean power analysis of the vibration signals is a relevant parameter to correlate with the tool wear. Ragai et al. [28] have correlated the turning process parameters with cutting tool vibration and energy consumption. The authors concluded that the cutting speed showed a substantial impact on tool vibration response while the change in feed rate affected the energy consumption in machining operation. Sivalingam et al. [29] examined the

impact of MQL technique on cutting tool vibration, surface integrity, and tool life while turning Inconel 718 steel. The machining performance parameters were evaluated in a dry and MQL cutting environment. The authors highlighted that the MQL technique significantly minimized the tool which resulted in lesser tool vibration amplitude and an improved surface finish than that of the dry cutting condition.

It is perceived from the review of various literature that the application of vegetable oils can enhance machining performance. However, limited research articles have addressed machinability in terms of crater wear depth  $K_T$ , cutting tool vibration, cutting temperature with IR thermography, and 3D topography of the machined surfaces. Hence, the primary objective of this study is to evaluate the effects of vegetable oil along with MQL technique on the machinability of AISI-1040 steel. The presence of more than 90% molecular weight of saturated fatty acids within the coconut oil (CO) and the highest concentration of lauric acids compared to any other vegetable oil, makes it a special category of vegetable oil known as lauric oils [30–32]. The CO also consists of superior oxidative and thermal stability compared to other commonly used vegetable oils which motivated us to choose it as a cutting fluid. Thus, the experimental investigation was conducted to analyze the performance of CO during the machining of AISI-1040 steel. The objective was to present a comparative analysis of different cutting conditions, namely dry, flood, MQL with mineral-based oil (MQL-MO), and MQL with coconut oil (MQL-CO). Several parameters were assessed to evaluate the machining performance, including tool flank wear, auxiliary flank wear, crater wear, surface finish, cutting temperature, tool vibration, chip morphology, and sustainability. Through this investigation, we aimed to provide insights into the potential benefits and effectiveness of CO-based MQL in enhancing the machinability of AISI-1040 steel during the turning process. The comprehensive analysis of various performance parameters provided valuable information to compare the performance of MQL-CO with other commonly used cutting methods for optimizing machining processes.

### 1.1 Cooling and lubricating mechanism of MQL-CO during the metal-cutting operation

The frictional interaction of workpiece-tool-chip surfaces and the permanent deformation of work material generate a large amount of heat during the metal-cutting process. The majority of the heat generated is dispersed through the chips  $Q_{c-t}$  and the heat remains at workpiece-tool interface is  $Q_{w-t}$  as shown in Fig. 1. When the CO is allowed to flow with MQL technique, high-pressurized micro-droplets of CO are impinged directly in the tool-workpiece interaction zone. The high content of saturated fatty acids present in the CO offered higher viscosity which resulted in longer retention

**Fig. 1** Schematic representation of interacting surfaces with vegetable oil molecules

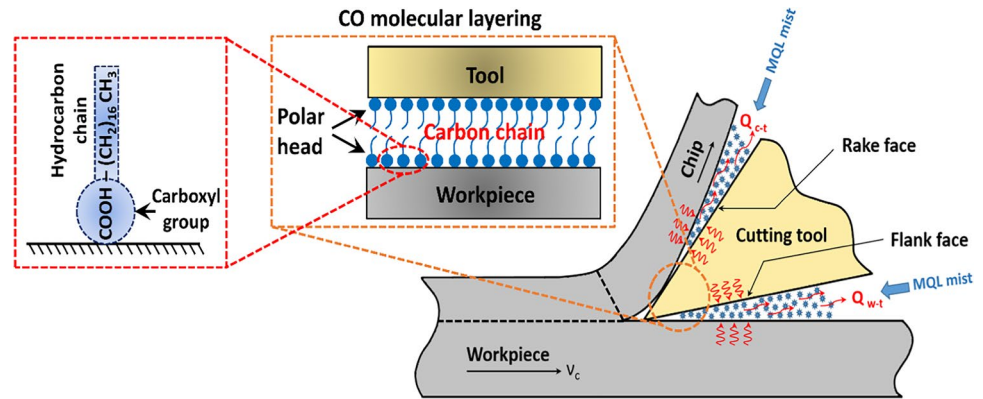


**Table 1** Physical properties of coconut oil [37]

Specifications	Range
Saturated fatty acids	90–94%
Unsaturated fatty acids	6–10%
Viscosity index (VI)	142
Viscosity in cSt at 40 °C	28.56
Viscosity in cSt at 100 °C	6.76
Refractive index at 25 °C	1.448–1.450
Specific gravity at 25/25 °C	0.915
Flash point (°C)	278
Cloud point (°C)	27
Melting point (°C)	21
Pour point (°C)	20

**Table 2** Chemical composition of coconut oil [38]

Component	Fraction (%)
Lauric acid (C 12:0)*	51.0
Myristic acid (C 14:0)	18.5
Caprylic acid (C 8:0)	9.5
Palmitic acid (C 16:0)	7.5
Oleic acid (C 18:1)	5.0
Capric acid (C 10:0)	4.5
Stearic acid (C 18:0)	3.0
Linoleic acid (C 18:2)	1.0

(C XX:Y) represents a fatty acid chain, where XX indicates the number of carbon atoms and Y represents the number of double bonds

of lubricating film, therefore better lubricating performance [33]. The physical properties and chemical composition of CO are presented in Table 1 and Table 2. The CO possesses a straight-line backbone structure of molecular chains, which are arranged in a perpendicular direction to the surface providing a high strength to the lubricating film as depicted in Fig. 1. The formation of thick lubricating film on the workpiece-tool-chip interfaces resulted in the reduction

**Table 3** Mechanical and physical properties of AISI 1040 steel

Ultimate tensile strength [MPa]	Modulus of elasticity [GPa]	Density [kg/m <sup>3</sup> ]	Hardness [HV]	Melting point [°C]	Thermal conductivity [W/mK]
500–800	190–210	7850	199–258	1520	50.7

of friction and wear. Furthermore, the long chain structure of fatty acids provided a higher cohesion between the CO molecules, which facilitated greater load-bearing capacity of CO than mineral oil-based cutting fluids. The polar group present in the triglycerides of CO molecules showed better adsorption in the cutting region, and the micro-droplets entering between the interacting surfaces have excellent chemical and physical adsorption with the workpiece and tool. Thus, better cooling and lubricating performance can be achieved with CO as compared to mineral oil-based cutting fluids [34–36].

## 2 Materials and methods

### 2.1 Workpiece, machine, and cutting tool

In the experimental investigation, AISI 1040 steel was considered as the workpiece material with dimensions of Ø 65 mm and 450 mm in length. This grade of steel is widely used in the manufacturing of shafts, keys, couplings, bolts, nuts, etc. The mechanical and physical characteristics of the workpiece material are listed in Table 3. All the turning experiments were carried out on a PACTURN-360 center lathe driven by a 2.4 kW AC motor. A PVD-TiAlN/TiN coated rhombic ZCC carbide insert rigidly fastened on an ISO-designated (SDJCR 2020 K11 WIDAX) tool holder was utilized as a cutting tool. The complete specification of cutting tool insert is provided in Table 4.

A schematic illustration of the experimental procedure is depicted in Fig. 2. The turning experiments were performed

**Table 4** Specification details of cutting tool insert

Parameters	Values
Manufacturers with ISO designation	ZCC cutting tool-DCMT11T304
Model	YBC251
Coating	PVD-TiAN coated
Shape	Rhombic- 2 sided
Major cutting-edge angle	55°
Clearance angle	7°
Nose radius	0.4 mm
Cutting edge length	11.6 mm
Insert thickness	3.97 mm
Corner radius	0.8 mm
Fixing hole diameter	4.4 mm
Inscribed circle diameter	9.525 mm

under four distinct cutting conditions, namely dry, flood, MQL with mineral oil-based cutting fluid (MQL-MO), and MQL with coconut oil (MQL-CO). Servo-cut soluble mineral oil (6–8% concentrated) diluted in pure water was utilized as a cutting fluid for flood pouring and MQL-MO cutting environments. In the flood-cutting condition, coolant was supplied to the cutting region with a gravity feed setup in which cutting fluid was kept in a container and placed over the machine tool at a height of 3 meters. The container was open to the atmosphere; hence the flow of cutting fluid was because of its self-weight and atmospheric pressure. A flow-adjusting valve was used to regulate the flow rate. During the trials, it was noted that for selected cutting parameters, a flow rate of 10 ml/min is adequate. The MQL setup was configured to 4–6 bar compressor pressure and a flow rate of 50 ml/h. In MQL, the coolant/lubricant was sprayed through a brass nozzle of Ø1 mm at a spray angle of 45° and 50 mm apart from the cutting region. The pictorial representation of an experimental set-up is shown in Fig. 3.

In order to effectively evaluate the machining performance, the turning experiments were carried out for over 50 minutes of cutting operation under selected cutting conditions. For each condition, a fresh cutting tool insert was utilized, and after every 10 minutes of cutting operation tool flank wear was measured. The required feed, speed, and depth of cut were selected based on preliminary experiments and the tool maker's recommendation. The machining parameters considered in this study are presented in Table 5.

## 2.2 Measurement techniques

A USB digital microscope AM 4113ZT (Dino-Lite) was adopted to evaluate the development of flank wear on the tool inserts. The tool wear mechanism and chip morphology were analyzed by using a field emission scanning electron

microscope (FE-SEM; Zeiss LEO440). The crater wear depth was analyzed with a 3D optical profilometer. The surface roughness was measured with the help of TESA rugosurf 10-G gage. The average surface roughness value ( $R_a$ ) was measured along the axial direction of the machined surface and same was considered to evaluate the surface finish quality. The 3D surface topography of the machined surface was also obtained using a phase-view optical profilometer. To acquire the cutting tool vibration in the tangential direction of the workpiece rotation, a uniaxial accelerometer sensor (CTC AC 102) with a sensitivity of 100.92 mV/g was mounted with the help of a magnetic stud on the top surface of the tool holder. The accelerometer was coupled with a dewetron data acquisition system (DEWE 43 A) to amplify the acceleration signals. The amplified voltages were then sampled using a computer through DeweSoft X2. The vibration data acquired during turning operation consisted of a tangential component of acceleration sampled at a frequency of 10 kHz.

### 2.2.1 Assessment of cutting temperature with IR thermography

The heat transfer effects of radiation during the machining can be analyzed by using IR thermography. The thermogram plots obtained by using an IR technique can be utilized to assess the cutting temperature. In IR thermography, infrared detectors are used to absorb the infrared radiation emitted during the metal-cutting process without coming into contact with the test specimen [39]. The temperature values below the visible light spectrum can be measured by using an infrared camera. The estimation of thermal radiation from the test object is carried out by using the “Stefan-Boltzmann law; which states that the total radiation emitted by a body is directly proportional to the fourth power of its absolute temperature,” given in Eq. 1 [40].

$$P = \epsilon \sigma T^4 \quad (1)$$

where  $P$ -total power radiated (Watts),  $\epsilon$ -emissivity of the material,  $\sigma = 5.67 \times 10^{-8} \text{ W/m}^2\text{K}^4$  (Stefan-Boltzmann's constant),  $T$ -absolute temperature of the body (Kelvin) respectively.

The workpiece-tool-chip interface temperature was obtained by using a Fluke TiX580 infrared camera with an optical resolution of 640×480. Its temperature measurement ranges from –20 to 1000 °C with an accuracy of  $\pm 2$  °C. Figure 4 depicts the temperature measurement setup with IR thermal imager. Firstly, the IR camera was calibrated with the help of a K-type thermocouple and IR temperature gun to minimize the errors. Then, it was utilized to assess the cutting zone temperature. The IR camera generates a thermogram of the cutting region with



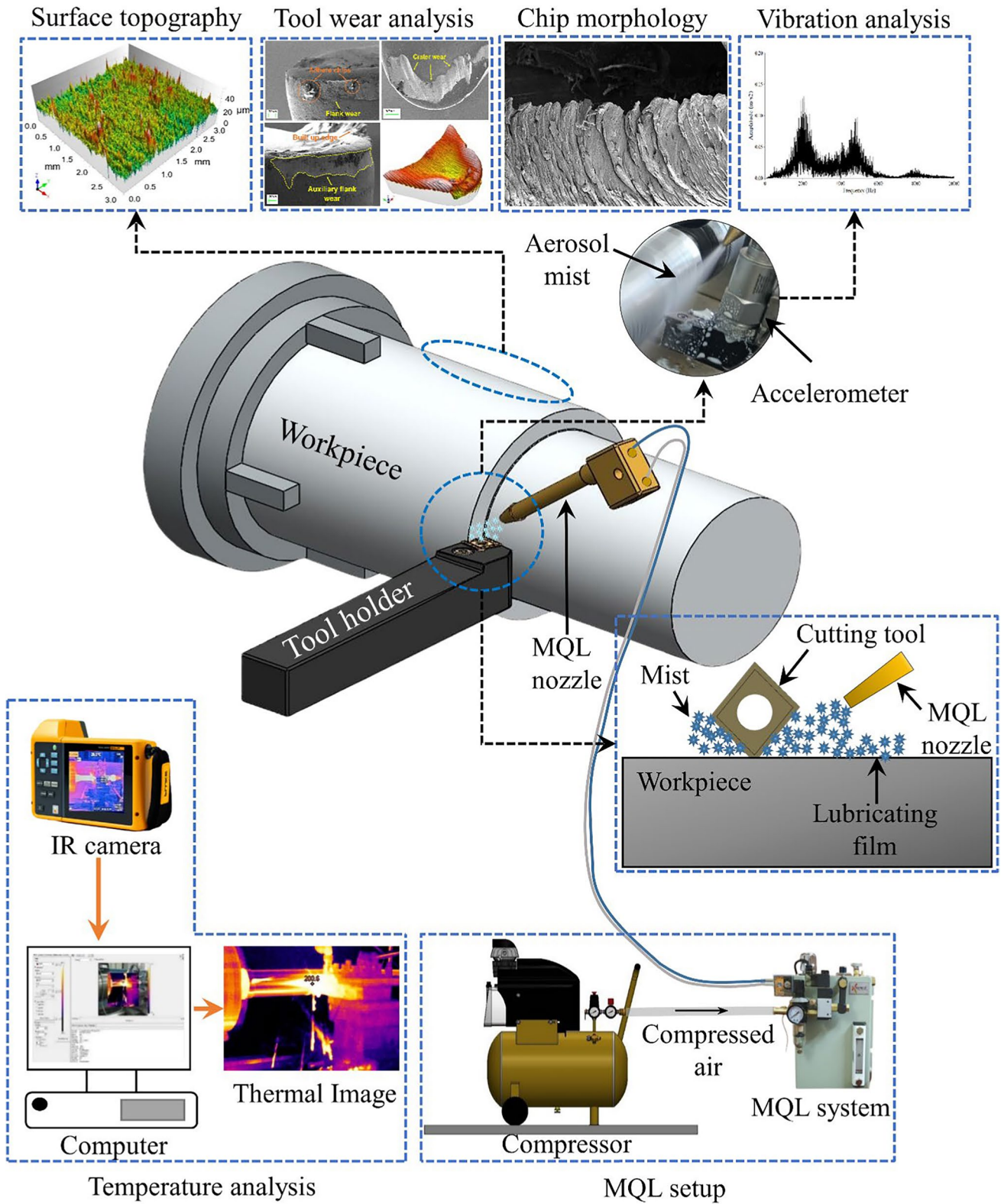


Fig. 2 Schematic illustration of experimental setup and workflow

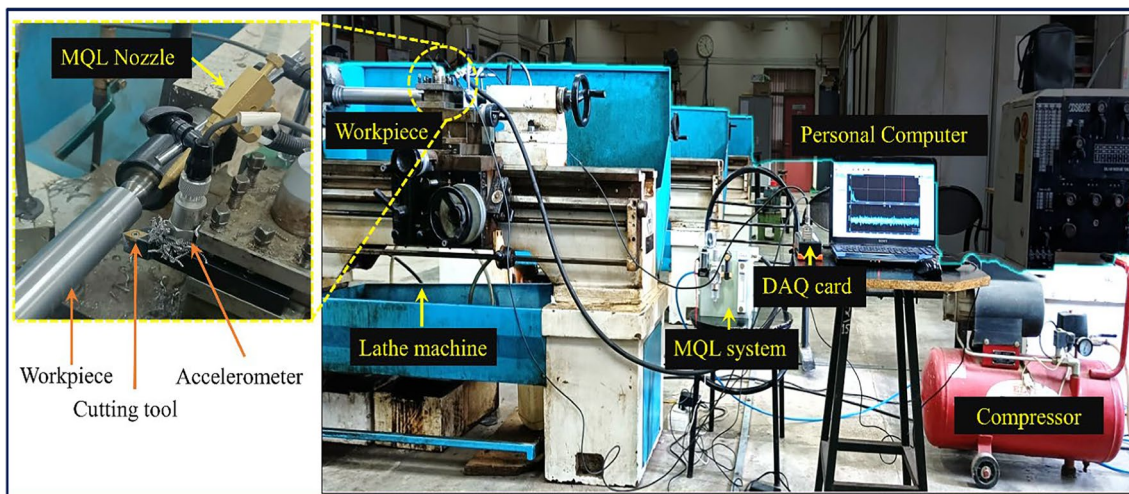


Fig. 3 Pictorial representation of an experimental setup

Table 5 Technical specification of work material, cutting parameters, and cooling conditions

Category	Specification
Machine tool	PACTURN-360 center lathe (2.4 kW, spindle speed: 45-1800 RPM)
Material	AISI 1040 steel (C = 0.36–0.45%, Mn = 0.6–1%, Si = 0.2–0.3%, S = 0.025%, P = 0.015%)
Feed rate, $f$ (mm/rev)	0.10
Cutting speed, $v_c$ (m/min)	125
Depth of cut, $a_p$ (mm)	1
Cutting conditions	Dry, flood, MQL-MO, and MQL-CO
Flow rate	10 ml/min (flood pouring); 50 ml/h (MQL)

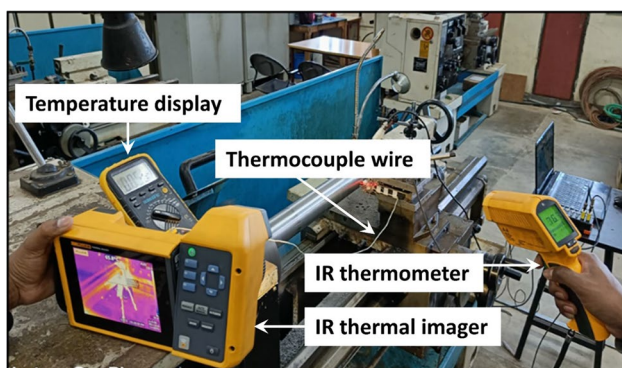


Fig. 4 Temperature measurement with IR thermal camera during the turning operation

distinct color-coded signposts. This thermogram depicts temperature gradients on the workpiece-tool-chip interface without interrupting the heat flow in the machining process. The thermogram was then post-processed by using SmartView software to acquire the cutting temperature.

### 3 Results and discussion

#### 3.1 Wettability analysis

The capability of a liquid to adhere on a surface can be determined by its wettability. The wettability is represented by the wetting angle formed by the liquid medium at the solid-liquid-gas phase interface. It can be controlled by the intrinsic characteristics of the liquid medium, surface texture, and thermal conditions of the substrate [30, 41]. The schematic representation of wetting angle measurement over a surface is illustrated in Fig. 5.

At thermodynamic equilibrium, the Young-Dupre Eq. 2 gives the wetting angle ( $\theta$ ) of a liquid medium placed on an ideal solid surface:

$$\cos \theta = \frac{\gamma_{sg} - \gamma_{sl}}{\gamma_{gl}} \tag{2}$$

where  $\gamma_{gl}$ ,  $\gamma_{sl}$ , and  $\gamma_{sg}$  indicates the surface tension of gas-liquid, solid-liquid, and solid-gas surfaces. Though, the Young-Dupre equation applies only to a perfect solid surface. The

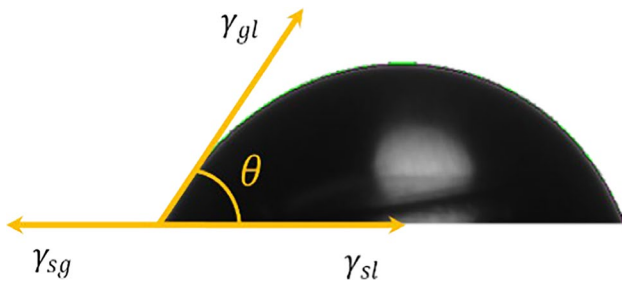


**Fig. 5** A graphical representation of wetting angle measurement at the solid-liquid interface

actual surface consists of different behaviour due to their surface properties. So, the Wenzel equation provides the wetting angle on a real surface formed by a liquid medium which is given by Eq. 3.

$$\cos \theta_w = r \cos \theta \quad (3)$$

where the wetting angle measured on an actual surface denoted by  $\theta_w$  and the average surface roughness is indicated by  $r$ . The value of  $r$  is unity for ideal surfaces, whereas it would be always greater than one for actual surfaces. Practically, the liquid wets the solid substrate only when  $\theta_w$  is lesser than  $90^\circ$ . On the other hand, when  $\theta_w$  is greater than  $90^\circ$ , the liquid will not wet the solid surface.

For the wetting angle measurement, a droplet volume of  $10 \mu\text{l}$  was taken with the help of a microliter syringe at room temperature and dropped over a tungsten carbide substrate having a surface roughness (Ra) of  $0.45 \mu\text{m}$ . The wetting angle was then measured by using a contact angle goniometer. The measured wetting angle of pure water, mineral oil, and coconut oil are  $75.4^\circ$ ,  $68.1^\circ$ , and  $33.7^\circ$  as depicted in Fig. 6. It is observed that the wetting angle of CO is much lower than that of MO and pure water. The lower wetting angle of CO indicated the larger wetting area on the carbide substrate with respect to the droplet volume. This facilitates

a better lubricating performance of CO at the workpiece-tool-chip interaction region.

### 3.2 Wear analysis of tool flank surface

Machinability attributes which include cutting forces, tool vibration, and cutting temperature have a significant effect on the occurrence of tool wear in the machining process. The abrasion takes place on the cutting edge of a tool insert and freshly cut workpiece material resulted in flank wear. The flank wear which occurs on the major cutting edge and the minor cutting edge of the tool insert is termed as flank wear and auxiliary flank wear respectively [31, 32]. Furthermore, the flank wear is categorized into average flank wear ( $V_{Bavg}$ ) and maximum flank wear ( $V_{Bmax}$ ). The actual cutting action takes place from the flank surface of the tool insert, while the auxiliary flank surface influences the dimensional deviation and surface finish quality of the machined workpiece [42]. The occurrence of various types of wear on the cutting tool insert is depicted in Fig. 7.

SEM micrographs of the flank surface and auxiliary flank surface of the cutting tool inserts under distinct cutting conditions are depicted in Fig. 8. Flank wear developed on the flank surface of the tool increased gradually with the increase in machining time. The adhesive and abrasive wear mechanism was dominant in the dry cutting leading to the adhered chips and built-up edge formation on the cutting tool inserts as shown in Fig. 8a and b. This can be correlated to the high cutting temperature in the absence of coolant. However, in a flood-cutting environment, some amount of heat is dissipated by the application of coolant, which does not penetrate the workpiece-tool interaction zone. This results in notch wear on the flank and auxiliary flank surface of the tool insert as shown in Fig. 8c and d. With the application of MQL technique, the pressurized mist directly impinges on the workpiece-tool-chip interfaces providing effective cooling in the cutting

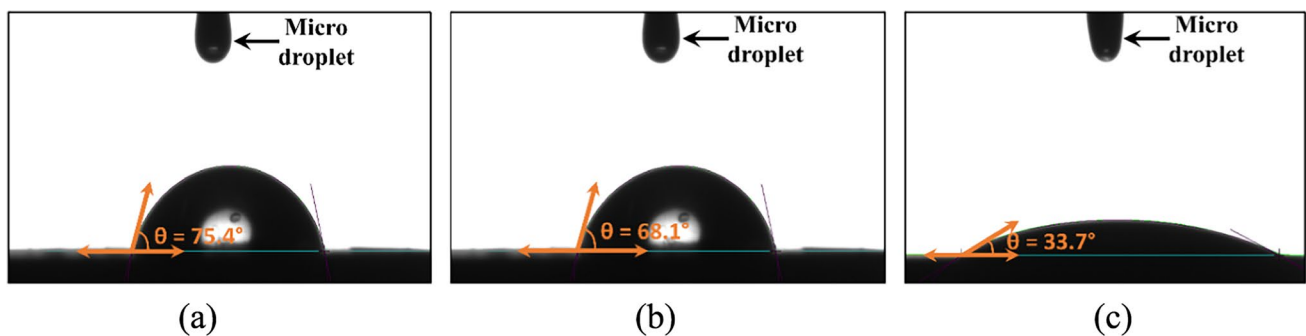
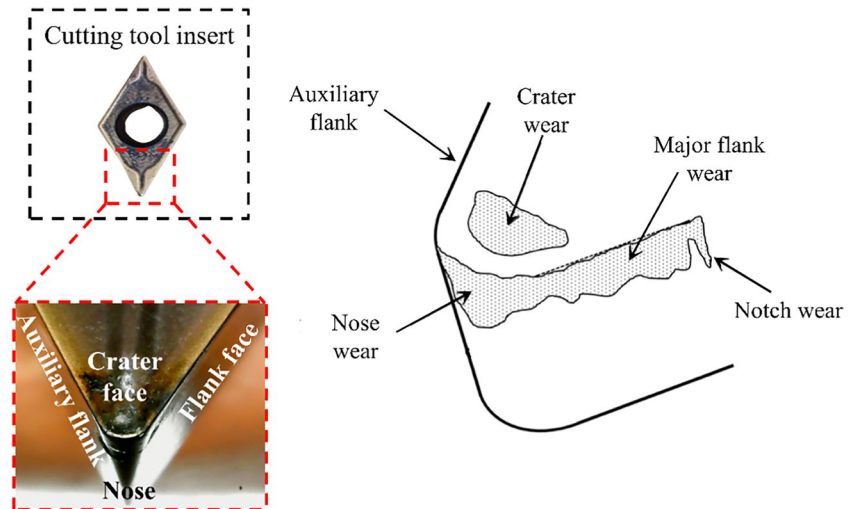


**Fig. 6** Wetting angle measurement of **a** pure water ( $\theta_w = 75.4^\circ$ ), **b** mineral oil ( $\theta_w = 68.1^\circ$ ), and **c** coconut oil ( $\theta_w = 33.7^\circ$ ) on the carbide surface of the cutting tool insert



**Fig. 7** Illustration of various types of tool wear: flank wear, crater wear, and notch wear



zone. The larger heat dissipation results in a significant reduction of tool wear and considerable improvement in the machining process.

In flood cooling, the temperature of the cutting zone is reduced by forced convection only, whereas the MQL technique does multiple contributions. Firstly, the mist generated by MQL wets the cutting surface with a layer of oil, which reduces friction. Secondly, the evaporation of coolant droplets enhances the heat transfer from the cutting zone. During turning with the MQL-MO cutting environment, mineral oil-based coolant does not provide sufficient lubrication between the tool-workpiece interface which might lead to an increase in the coefficient of friction. This can be the reason for adhered chip and larger tool wear in MQL-MO cutting condition when correlated with MQL-CO as depicted in Fig. 8e and f. It was noted that after 50 min of turning operation, lesser flank wear was observed in the MQL-CO cutting environment as depicted in Fig. 8g and h. This shows the effective cooling and lubrication capabilities of coconut oil. The tool flank wear obtained under MQL-CO cutting showed a significant reduction of 52%, 33%, and 17 % respectively in comparison with dry, flood, and MQL-MO cutting conditions.

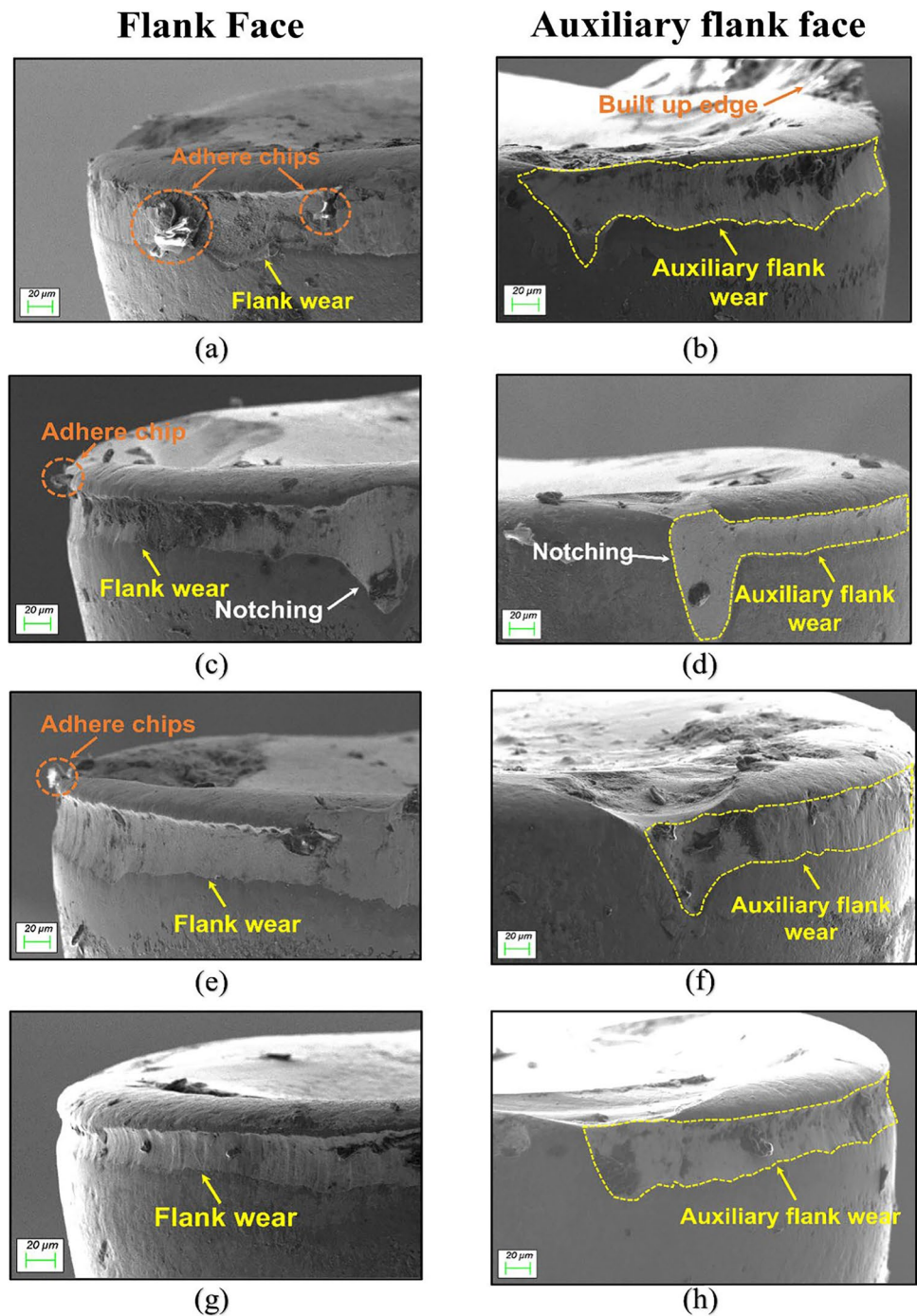
The maximum flank wear ( $V_{Bmax}$ ) and the average flank wear ( $V_{Bavg}$ ) generated on the cutting tool inserts and the variation of flank wear with the machining time under distinct cutting environments are depicted in Fig. 9a and b. The reduction in auxiliary flank wear can be attributed to the decrease in flank temperature which reduces abrasion and maintains tool hardness during the MQL cutting environment. Furthermore, a high-pressurized jet of CO impinges at the chip-tool contact interface, results in a notable reduction in flank surface wear of the cutting tool insert ascribed to its unique properties, viz., excellent lubricity, high thermal stability, high viscosity index, and greater oxidation stability.

### 3.3 Wear analysis of tool rake surface

The constant interaction among the chips and the tool surface interface causes crater wear on the rake surface of the cutting tool insert. The crater wear was observed at a particular distance from the cutting edge at which the chip strikes the crater surface of the tool insert. This striking can generate a high coefficient of friction resulting in high temperature at the chip-tool intersection zone. Based on the temperature distribution, abrasive, adhesive, and diffusion wear mechanisms are the principal causes of crater wear, which propagates on the crater surface of a tool insert [43]. The crater wear is assessed by measuring the crater wear depth  $K_{Tmax}$ .

SEM images of the rake surface and the corresponding 3D images observed under dry, flood, MQL-MO, and MQL-CO are depicted in Fig. 10. In dry cutting, a chip adhesion of the workpiece material with higher crater wear was observed as shown in Fig. 10a and b. During the flood-cutting environment, due to the lack of penetration of coolant at the chip-tool interaction zone results in considerable crater wear as shown in Fig. 10c and d. While the MQL-assisted cutting environment, a high-pressure jet of coolant/lubricant efficiently removed the chip from the cutting zone resulting in shorter interaction of the chip with the tool rake face. This resulted in lesser friction between chip-tool interaction surfaces resulted in comparatively lesser crater wear which is clearly depicted in Fig. 10e–h. A moderate crater wear that appeared on the crater surface has a negligible effect on machining performance. However, the crater formation led to a high effective rake angle of the cutting tool insert causing a reduction in cutting forces. On the other hand, excessive crater wear depth weakens the cutting edge resulting in failure or fracture of the tool cutting edge. The extent of crater wear is measured by the crater

**Fig. 8** SEM micrographs of the flank face and auxiliary flank face of the cutting tool under distinct cutting conditions: **a, b** dry, **c, d** flood, **e, f** MQL-MO, and **g, j** MQL-CO



depth  $K_T$ . The variation of crater wear depth  $K_T$  along the path drawn on rake surface of the cutting tool insert is depicted in Fig. 11. It was observed that the crater depth is not uniform along the rake face of the tool. A considerable reduction of 58%, 37%, and 15% was observed in the crater wear depth under MQL-CO cutting in comparison with dry, flood, and MQL-MO cutting conditions.

### 3.4 The influence of MQL-CO on the surface topography

The average surface roughness parameter ( $R_a$ ) of a material represents the height deviation of a surface relative to the mean line. The surface finish of the workpiece machined by using various machining processes, viz., turning, milling,

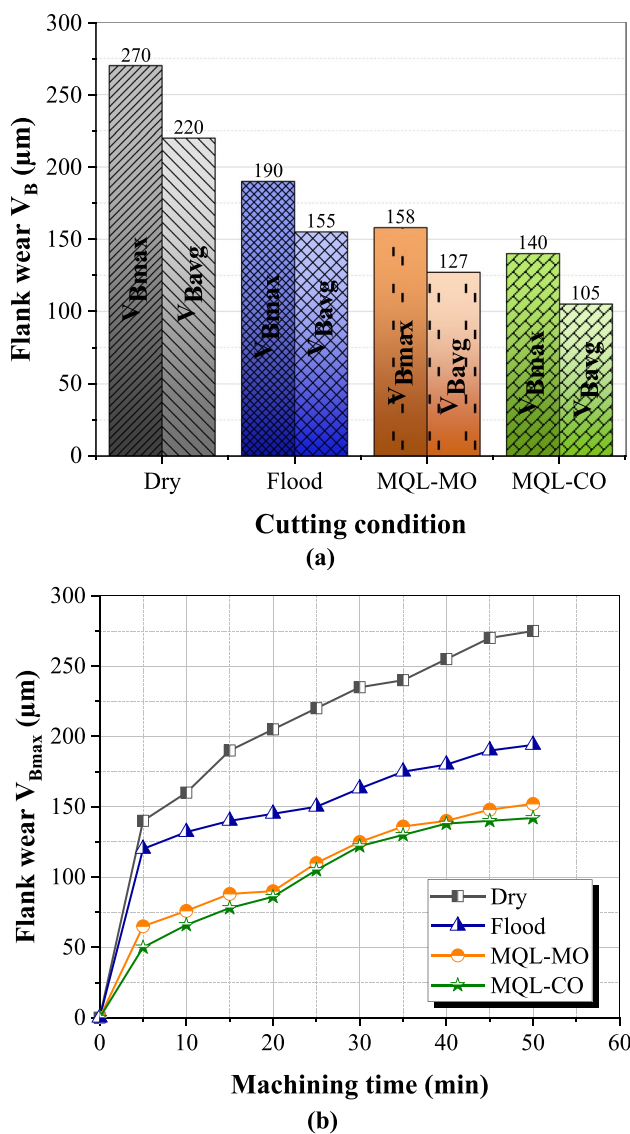


**Fig. 9** Flank wear observed under distinct cutting conditions. **a** Maximum flank wear  $V_{Bmax}$  and average flank wear  $V_{Bavg}$  and **b** flank wear  $V_{Bmax}$  progression with machining time

grinding, is assessed by using  $R_a$  values which affect the machining performance, tool life, and manufacturing cost [44]. Surface finish mainly depends on feed rate, cutting speed, and depth of cut during the metal cutting operation. Also, the application of the coolant/lubricant plays a crucial role in enhancing the machined surface quality [45].

The microscopic images of the machined surface and their 3D topographies under distinct cutting conditions are depicted in Fig. 12. Analysing the surface topography of the machined component will significantly contribute to enhancing the tribological behavior of the coolant/lubricant [46]. It was observed that the MQL-CO cutting environment has the lowest peak-to-valley height while the dry cutting has the highest. In a flood-cutting environment, this peak-to-valley

height is lower than that in dry cutting, this value further reduces under MQL cutting conditions. The tribological interaction of the chip-tool interface will affect the surface topography of the machined component. Furthermore, uneven feed marks and debris particles were reduced with the application of MQL, which results in a better surface finish of the machined component.

The variation in surface roughness values  $R_a$  of the machined workpiece under selected cutting conditions is depicted in Fig. 13. The application of the MQL results in a considerable reduction in  $R_a$  values. The MQL cutting environment had lower surface roughness values compared to dry and flood-cutting conditions. Further, the implementation of CO with MQL significantly reduces surface roughness. A better surface finish with a reduction of 48%, 24%, and 22% was obtained with MQL-CO cutting when correlated with dry, flood, and MQL-MO cutting conditions. The effective cooling and lubrication effect of MQL-CO results in chip curling and enhanced lubricant penetration into the cutting zone is primarily responsible for the decrease in surface roughness.

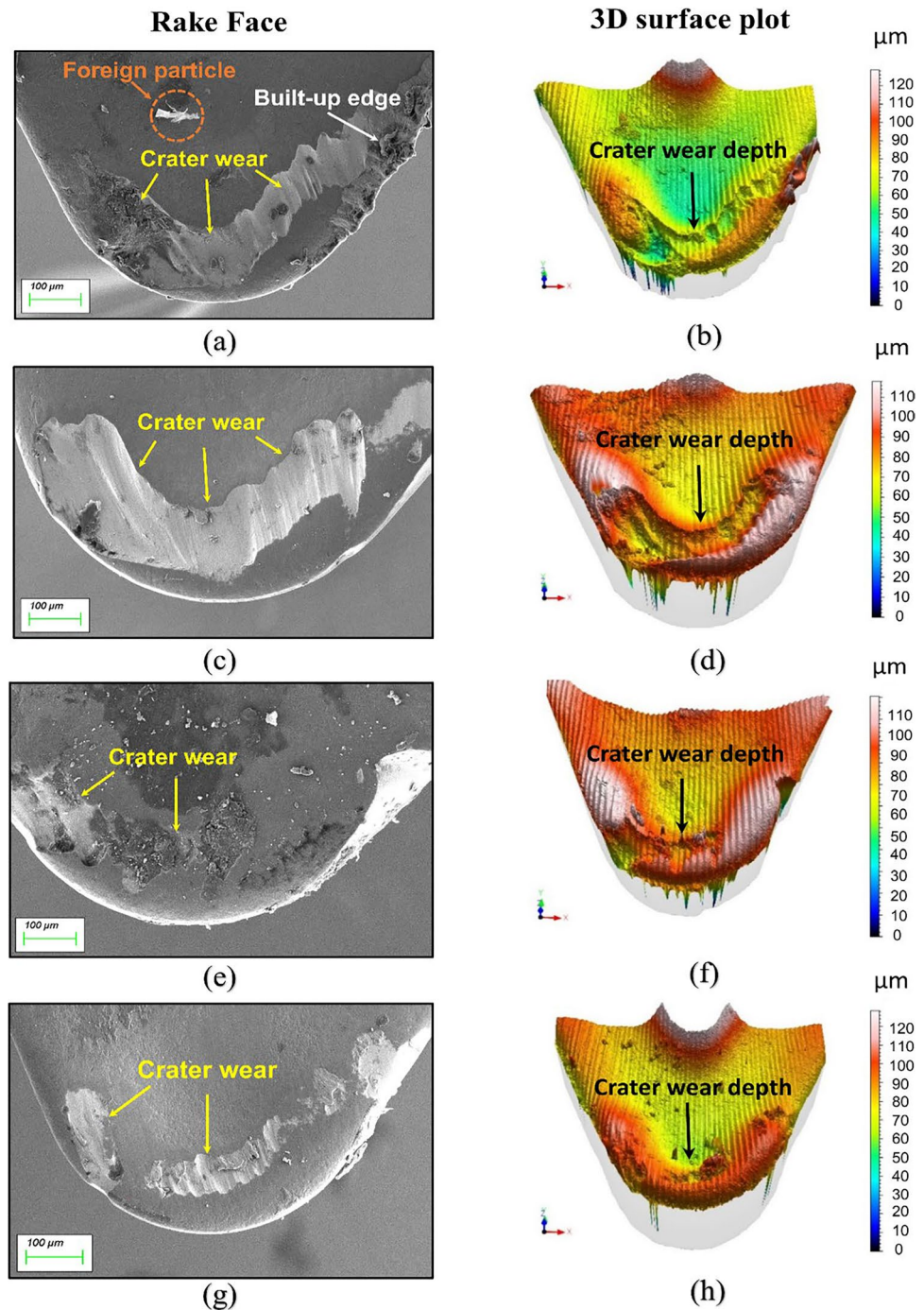
### 3.5 The influence of MQL-CO on the cutting temperature

The measurement of cutting zone temperature was performed to examine the tribological influence of CO with MQL on the friction between tool-workpiece interfaces. During turning operation, the workpiece-tool-chip temperature was obtained by using an IR camera. The IR thermal images of the cutting zone were acquired from a constant measuring distance. IR Thermographic images of the workpiece-tool-chip interface under distinct cutting conditions are depicted in Fig. 14. Results showed the highest cutting temperature of 290 °C during the dry turning operation due to the severe heat generation in the cutting zone. As the coolant is allowed to flow in the cutting zone during a flood-cutting environment, it carried away the heat which significantly reduces the temperature to about 221 °C. On the other hand, when MQL is incorporated, the cooling action of the throttled air along with coolant further decreases the cutting zone temperature and washed away the chips which are carrying a large amount of heat from the cutting zone.

Variation of the cutting zone temperature values with respect to machining time obtained under distinct cutting conditions is depicted in Fig. 15. The cutting temperature increased with machining time irrespective of the application of coolant. In dry cutting, the temperature values increase rapidly with time due to the continuous interaction of chip-tool-workpiece interfaces. While under the application of coolant, a large amount of heat is carried away and temperature increases gradually with time. The cutting temperature was considerably reduced



**Fig. 10** SEM micrographs and 3D surface plot of rake surface of cutting tool insert illustrating crater wear under distinct cutting conditions: **a, b** dry, **c, d** flood, **e, f** MQL-MO, and **g, h** MQL-CO



by 40%, 22%, and 13% under MQL-CO cutting in comparison with dry, flood, and MQL-MO cutting conditions. The lowest cutting zone temperature in MQL-CO is owing to the formation of oil film between the interacting surfaces and its constituents results in excellent lubricity. Also, the presence of polar head molecules shows a great chemical affinity for metal surfaces by attaching themselves perpendicularly along the metal

surface like magnets. This generates a thick and dense film layer of lubricant on the metal surface which further reduces the friction between tool-workpiece interfaces. From Fig. 15, it can be seen that after 10 min. of machining operation under MQL, the temperature values were always constant with respect to the machining time which can be attributed to better heat transfer coefficient of CO than that of MO.



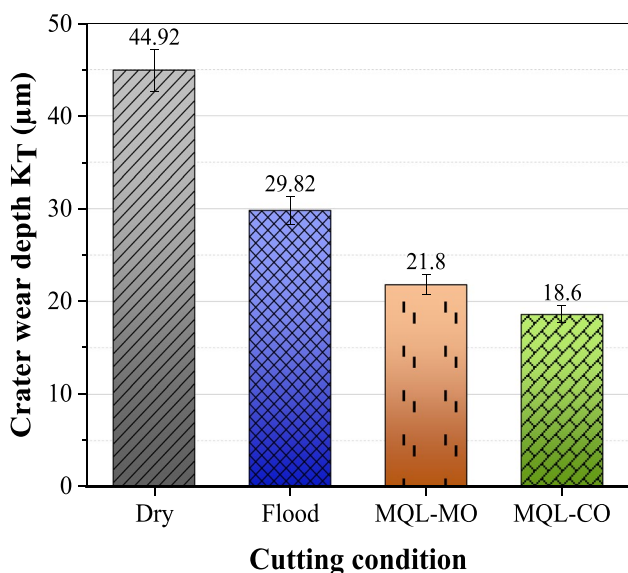


Fig. 11 Crater wear depth ( $K_T$ ) under distinct cutting conditions

### 3.6 The influence of MQL-CO on cutting tool vibration

In the metal cutting process, the dynamic interaction between the cutting tool and an elastic system results in the relative displacement of the tool and the workpiece leading to the cutting tool vibration. Vibration in metal cutting is one of the most prominent parameters, which influences machined surface quality, cutting forces, tool wear/life, and the residual stresses of the machined surface [47, 48]. Hence the monitoring and analysis of cutting tool vibration is of utmost importance during the metal-cutting process. The temporal waveform of vibration signal acquired during the cutting process is converted into frequency domain by using the Fourier transform (FT) function. FT indicates the vibration signal energy on frequency amplitudes in natural frequency region of the tool holder. This frequency amplitude indicates the tool wear severity with respect to the increase in flank wear/crater wear propagated on the cutting edges of the tool inserts [49]. The FT converts time domain signals into the frequency domain then analysis decomposes a signal into its frequency components to determine its relative strengths. The FFT of a time domain signal is given by Eq. 4.

$$F(\omega) = \int_{-\infty}^{\infty} x(t)e^{-j\omega t} dt \tag{4}$$

From the transform  $F(\omega)$ , the time domain signal can be obtained by inverse FT given by Eq. 5

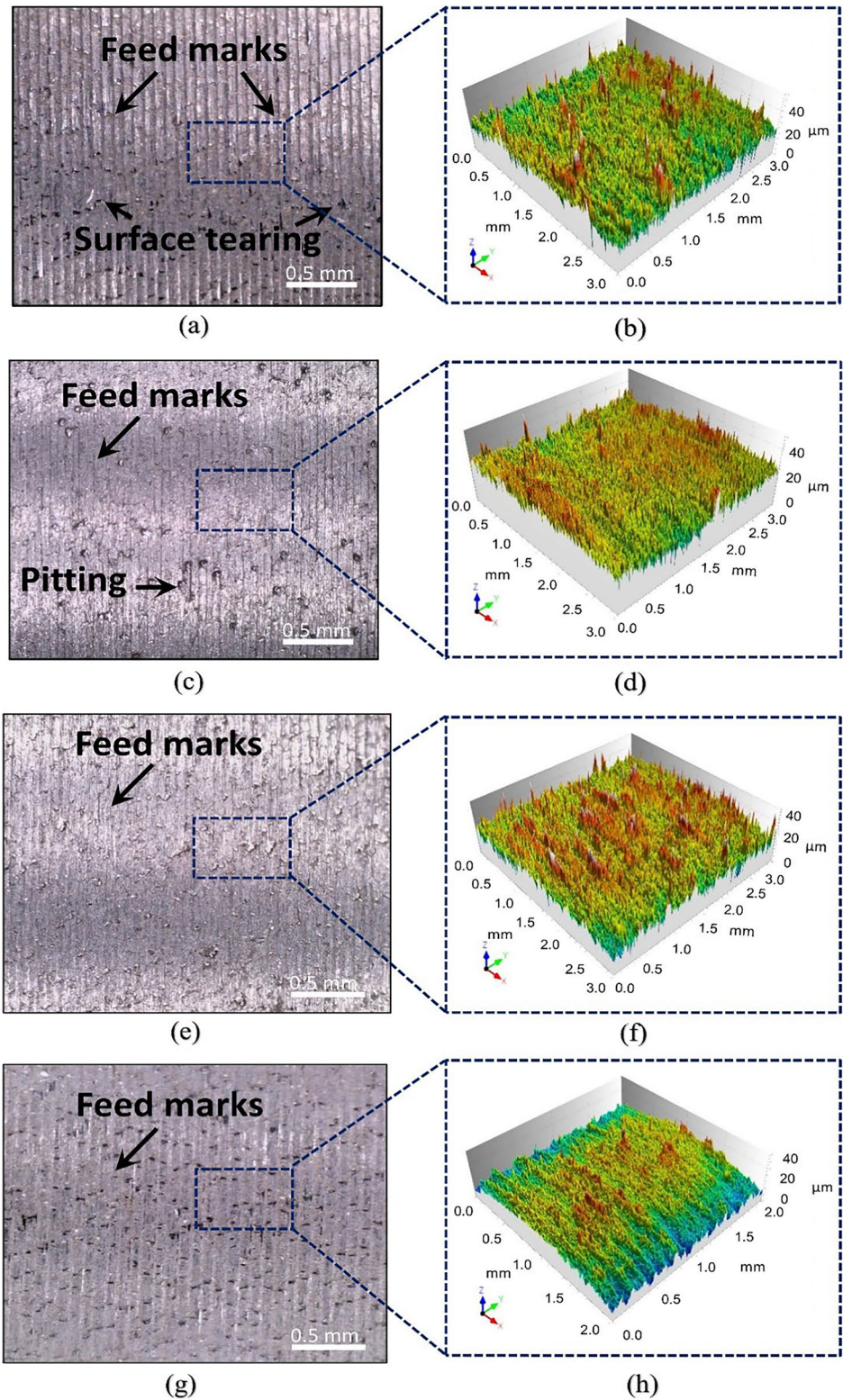
$$x(t) = \int_{-\infty}^{\infty} F(\omega)e^{j\omega t} d\omega \tag{5}$$

The vibration signals were acquired from the cutting tool holder to indicate wear occurred on the tool insert during the machining process. Figure 16a and d depict time waveforms of vibration signals acquired under dry, flood, MQL-MO, and MQL-CO cutting conditions respectively. The y-axis indicates acceleration amplitude in  $\text{m/sec}^2$  whereas the x-axis shows time in seconds. The time waveform obtained from dry and flood conditions showed higher vibration amplitudes than that of MQL-MO and MQL-CO conditions. These higher vibration levels can be attributed to the absence of cutting fluid which resulted in increased friction coefficient values between tool and workpiece during dry machining conditions. Whereas, in flood-cutting condition, though coolant is allowed to impinge on tool and workpiece interfaces, the quantity, pressure, and flow conditions fail to provide appropriate lubrication. As a result, an increase in friction values is observed in flood-cutting condition which intern causes higher vibration levels. The MQL provides a microjet of high-pressure coolant on the tool-workpiece interface. This microjet of coolant in the atomized form around 5 bar pressure penetrates into the tool-workpiece interface during machining, which resulted in better cooling and lubrication than that of dry and flood cutting conditions. Further, the mist particles of CO with high pressure and velocity impinge on tool-workpiece interfaces.

The CO molecules which consist of triglycerides form a strong protective layer on the tool-workpiece interface region which resulted in a considerable decrease in friction, wear, and temperature on the flank surface of a tool insert thereby causing a reduction in cutting forces, better surface finish, and favourable chip morphology than that of dry, flood, and MQL-MO machining conditions. A considerable reduction in friction between the flank face and machined work surface due to the MQL-CO condition led to minimizing wear on the tool edge thereby causing lower vibration levels. The vibration temporal waveform depicted in Fig. 16d indicates a significant reduction in the vibration amplitudes. Further, Fourier transform (FT) technique was used to convert the time waveform of acceleration signals into the frequency domain. The FT plot indicates fundamental resonant frequency bands which are associated with tool wear severity.

Figure 17a–d depict the FT plots of vibration signals acquired under dry, flood, MQL-MO, and MQL-CO respectively. The vibration amplitude in  $\text{m/sec}^2$  is shown on the x-axis and the frequency in Hz is indicated by y-axis. The fundamental resonant frequency band of the tool holder is shown around 2–4 kHz in Fig. 17a, which belongs to the dry cutting condition. The severe flank and crater wear were observed in dry cutting conditions

**Fig. 12** Machined surface and their 3D topographies under distinct cutting conditions



leading to an increase in vibration frequency amplitudes around 2kHz. Further, a significant reduction in tool wear was observed in flood, MQL-MO, and MQL-CO

respectively. A reduction in vibration frequency amplitudes at the fundamental resonant frequency region is shown in Fig. 17b–d.



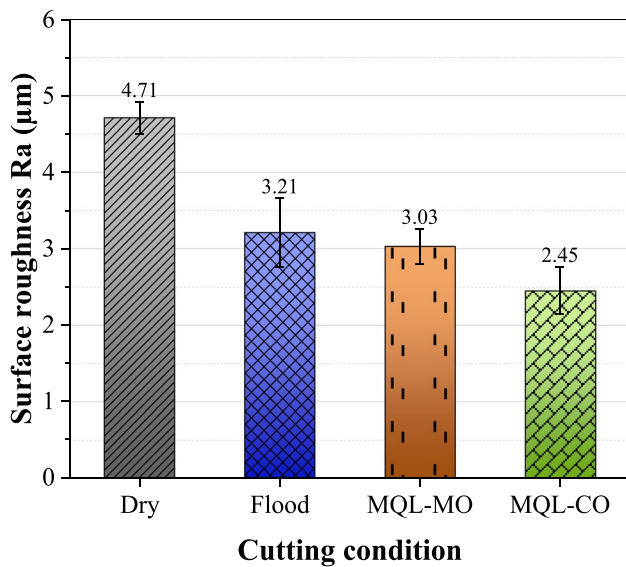


Fig. 13 Surface roughness variation under distinct cutting conditions

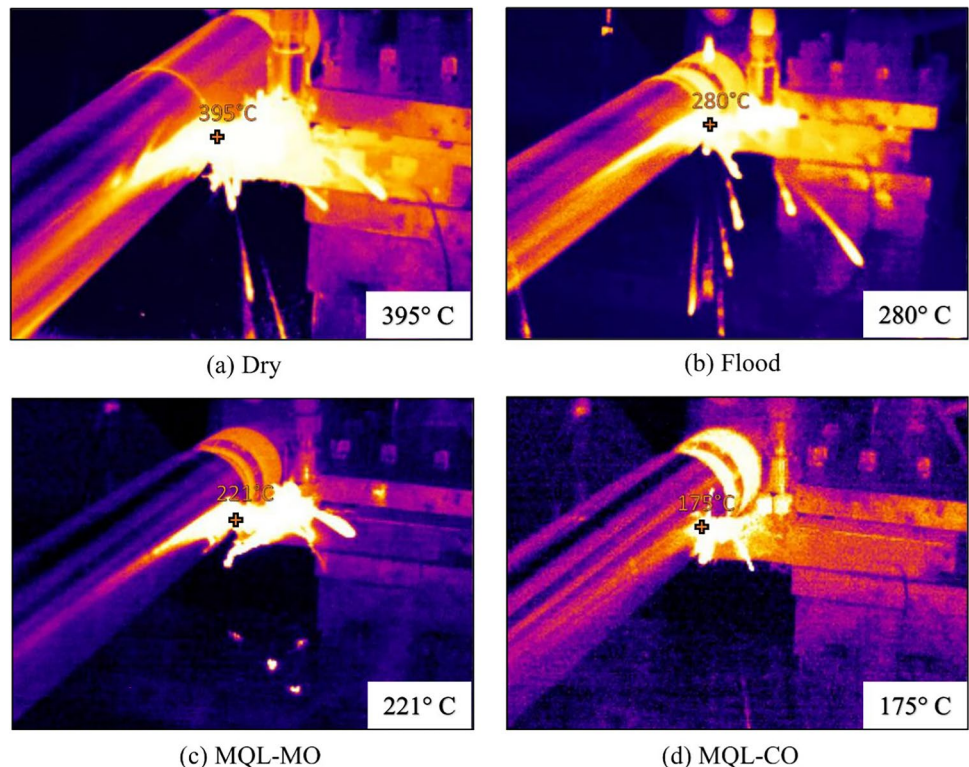
### 3.7 The influence of MQL-CO on chip morphology

The chip was generated due to the permanent deformation of work material during the metal-cutting process. The chips produced during machining also have a direct influence on machining parameters such as tool wear/life, surface finish quality, and cutting zone temperature [50]. The chips are

produced in various varieties of shapes and sizes depending on the cutting environment. A chip morphological study was conducted to investigate the tribological effects of cutting environment on the chip generation mechanism. The chip morphology provides essential information on the cutting mechanism which is closely associated with the surface waviness of the workpiece. To analyze the morphology of front and back sides of the chip, SEM images were obtained from the chip samples as depicted in Fig. 18a–d. The front side comprises of serrated rough edges generated due to the shearing action on work material. While back side of the chip surface slides over the rake face of the tool inserts. This sliding action generates a high frictional force and contact pressure between the chip-tool interface thereby resulting in a flat and clear back surface.

When the front side of the chips is evaluated, large serration is identified in the dry cutting condition, which implies a higher friction coefficient between chip-tool interfaces. On the other hand, small serration occurred under MQL-CO cutting condition shows the good lubricity of CO which results in the decrease of friction coefficient. When the back-side of the chip was evaluated, it is observed that significant scratches occurred under dry cutting, indicating the high friction coefficient between the chip and rake face of the tool. During the flood-machining environment, serration and scratches were present on the front and back sides of the chip surface as shown in Fig. 18b, which can be attributed to insufficient penetration of coolant in the tool-workpiece

Fig. 14 IR thermal images illustrating the cutting temperature under distinct cutting conditions



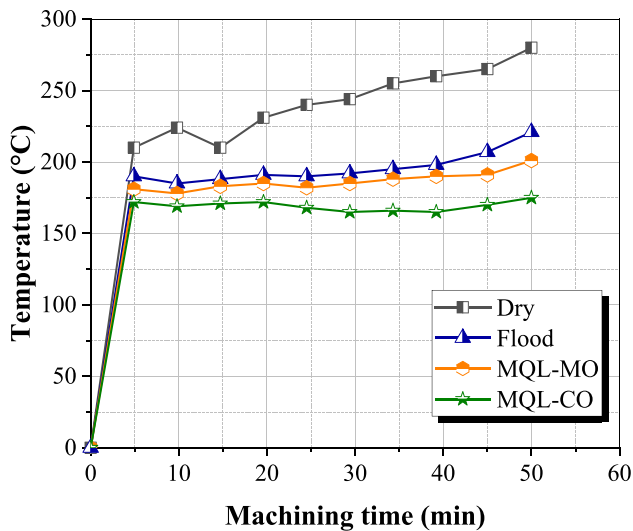
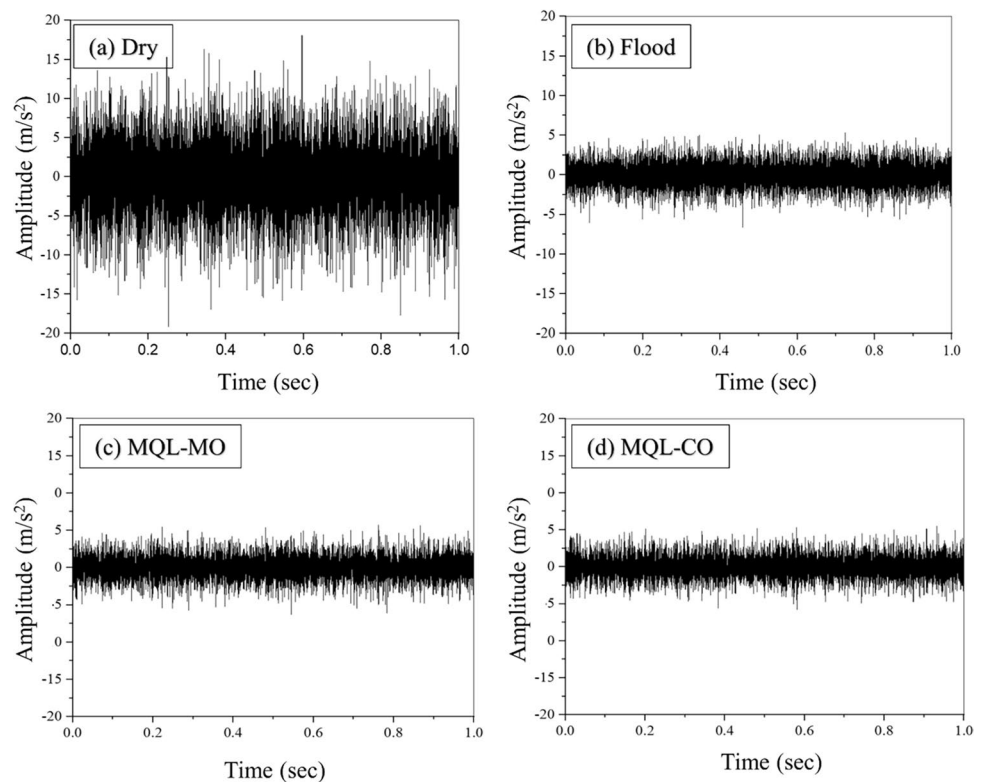


**Fig. 15** Cutting temperature variation with machining time under distinct cutting conditions

interface. On the other hand, front and back chip surfaces obtained under MQL-MO and MQL-CO are indicated in Fig. 18c and d respectively. A significant reduction in serration and scratches can be observed in the micrographs. The pressurized coolant droplet impinges on the tool and the workpiece resulting in a considerable reduction in friction and temperature. The MQL cutting environment led to superior lubricity and cooling, as a result, a flat and shiny

**Fig. 16** Cutting tool vibration spectra in the time domain under distinct cutting conditions



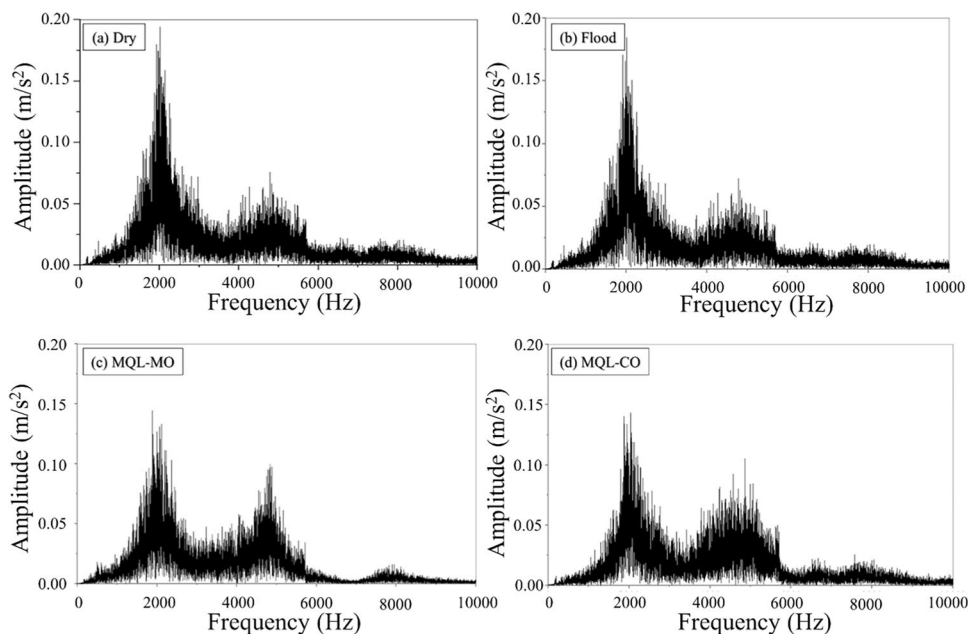
back face of the chip is observed in micrographs in Fig. 18c and d which contributed to better surface finish and extended tool life in turning operation.

#### 4 Sustainability assessment of cooling approaches

To develop and achieve sustainable machining, the health and environmental effects of the utilized cooling/lubrication approach must be addressed along with machining performance. The application of conventional fluids during flood cooling creates threat to human health due to the possibility of infectious diseases such as cancer, skin disorder, etc. Besides, large quantities of synthetic fluid used in flood cooling severely affect human health. In contrast, vegetable oils, including coconut oil, are derived as organic products from plant seeds and contain triglycerides with long chains of fatty acids. The direct exposure of the operator to these biodegradable oils does not create any health issues. Additionally, the application of vegetable oil through MQL possesses minimal effect. Traditional cutting fluids are a mixture of oils, water, and additional substances. The disposal of these cutting fluids causes serious environmental issues in the form of water and soil pollution. At the same time, coconut (vegetable) oil fulfills the sustainability criteria with its biodegradable and renewable nature and possesses significantly less toxicity. Also, conventional cutting fluids



**Fig. 17** Cutting tool vibration spectra in frequency domain under distinct cutting conditions: **a** Dry, **b** flood, **c** MQL-MO, **d** MQL-CO



demand separation and filtration processes for their recycling and disposal, thus consuming part of energy during lubrication. Whereas the minute quantity of vegetable oil supplied under MQL evaporates during machining and does not require separate measures for recycling and disposal.

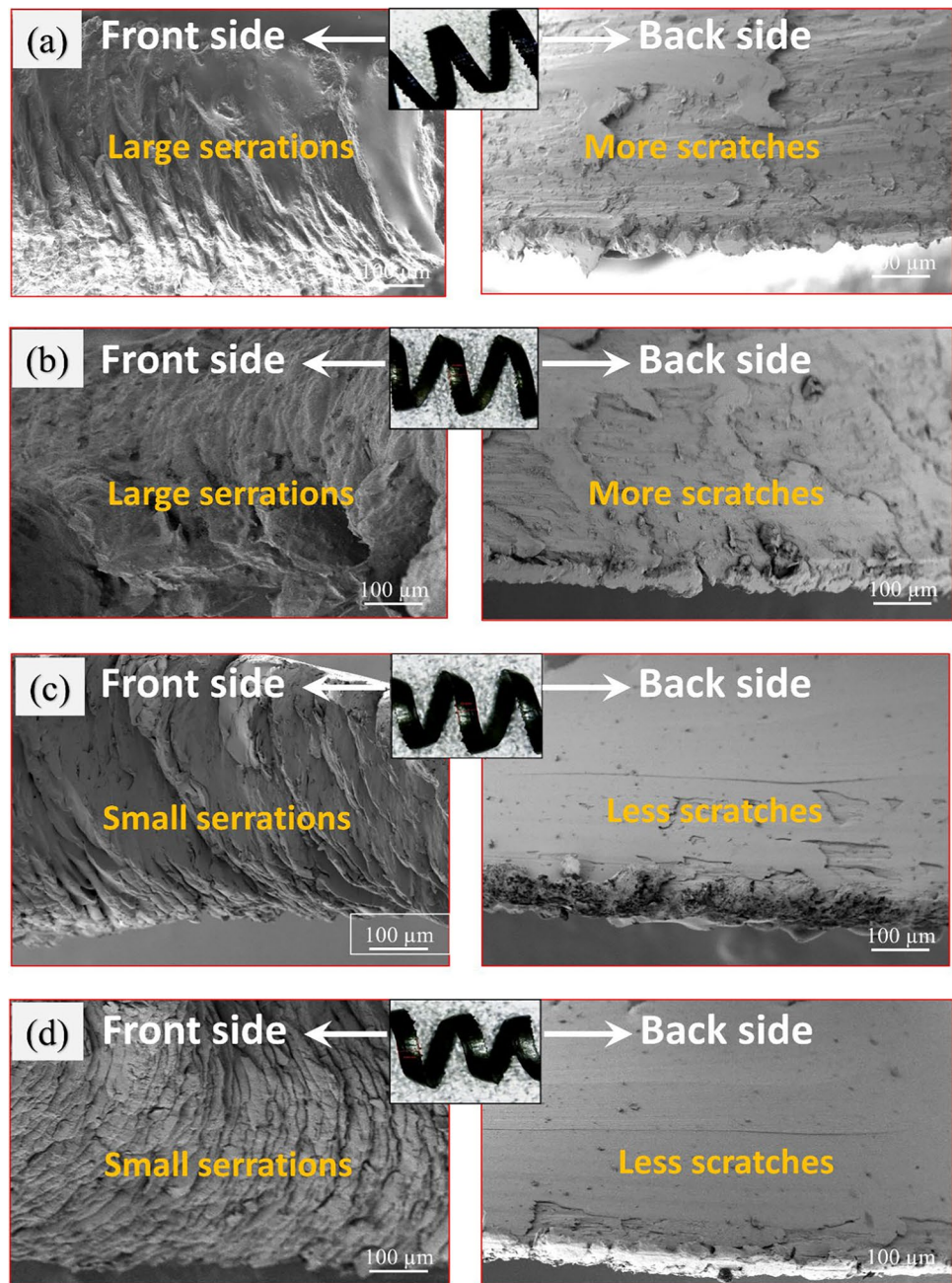
Sustainability assessment of cooling/lubrication techniques is essential to develop clean and environmentally benign machining processes. In addition to manufacturing aspects, the sustainability assessment involves the cost of coolants, the effect on the environment and workers' health, recycling and disposal needs, surface quality of the machined part, part cleaning requirements, etc. (Fig. 19).

Therefore, this work has made an effort to assess sustainability through the Pugh matrix approach. The Pugh matrix can be utilized to compare the available alternatives through pairwise comparison [51]. In the current work, the sustainability of the process under various cooling environments is evaluated by considering operator health, cost of coolant, environmental effect, part cleaning requirement, recycling and disposal needs, and surface quality. The weightage between  $-2$  and  $+2$  is considered to compare the parameters [52–54]. Hence,  $-2$  is assigned for poor results, and  $+2$  is considered for superior results for the selected criteria. Table 6 presents the assigned score for the selected alternatives.

Without using any coolant in dry machining, a score of  $+2$  is assigned for effect on operator health and environment. Whereas a score of  $-2$  is assigned to flood cooling as a large amount of cutting fluid is consumed during machining, which produces harmful emissions in the surrounding environment. A score of  $-1$  is considered for MQL-MO and MQL-MO as it has utilized the least amount of cutting fluid and created less harmful emissions

and effects on workers' health and environment. Machining under dry machining comes with cost-benefit related to the coolant and thus assigned with  $+2$ . In contrast, due to the excessive application of cutting fluid under flood cooling, a score of  $-2$  is considered. Also, it add-up the additional cost of cleaning and filtering. The application of MQL reduced the coolant requirement; thus,  $+1$  is considered. Further, dry machining without coolant requires no recycling and disposal and is assigned a score of  $+2$ . With the large quantity of cutting fluid used in flood cooling, separate recycling and disposal provision are needed during machining and assigned a score of  $-2$ . A small quantity of cutting fluid is applied during MQL and evaporates without any need for recycling and disposal and thus is considered with  $+2$ . Considerable efforts are required for part cleaning debris from the surface after operation in dry machining and assigned with a weight of  $-2$ . While MQL is assigned with a  $+1$  score as the application of compressed air blows away the debris and the cutting fluid with a small quantity evaporates during machining and hence requires little cleaning. A comparison of surface quality in the earlier section showed the superiority of MQL-CO compared to dry and flood cooling; therefore, a score of  $+2$  is assigned. From the total score presented in Table 6, MQL-CO has achieved the highest score (6) followed by MQL-MO (5), dry machining (4), and flood cooling ( $-8$ ). It can be summarized that applying MQL with coconut oil is a feasible alternative to achieve machining with less impact on cost, the health of the operator, and the environment. However, to make such a choice, further efforts can be made in this direction by considering total machining and energy cost, carbon emissions, etc.

**Fig. 18** SEM micrographs of the front and back surface of the chip



## 5 Conclusion

The objective of this investigation is to evaluate the impact of different cutting conditions during the machining of AISI-1040 steel in terms of flank wear, crater wear surface roughness, cutting temperature, cutting tool vibration, and chip morphology. The following conclusions are drawn based on experimental results:

- 1 The coconut oil has shown a much lesser contact angle than mineral-based oil which resulted in the effective wetting capability of coconut oil during the machining process.
- 2 The adhesion and abrasion wear mechanisms were observed on the cutting tool inserts while machining in the selected cutting conditions. The maximum flank wear was reduced by 48%, 26%, and 12% while the average flank wear was reduced by 52%, 32%, and 21% with MQL-CO cutting when compared with dry, flood, and MQL-MO cutting conditions.
- 3 A significant reduction of 59%, 38%, and 15% in crater wear depth was observed under MQL-CO in comparison

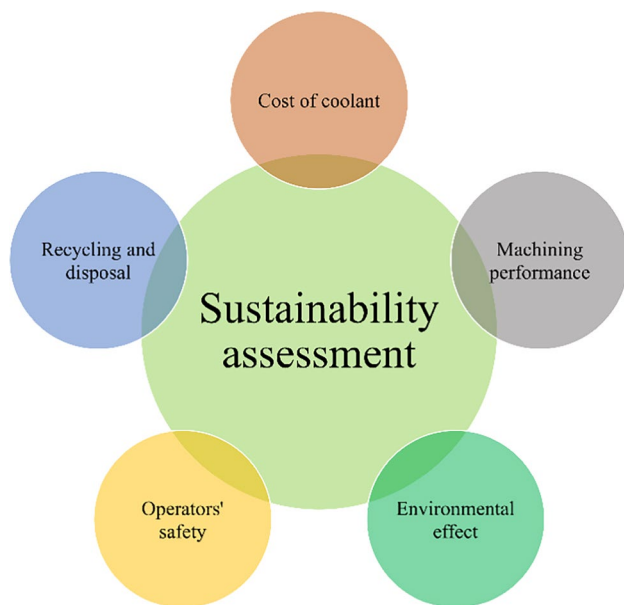


**Fig. 19** Elements for sustainability assessment

**Table 6** Comparison of different cooling/lubrication approaches

Criteria	Dry	Flood	MQL-MO	MQL-CO
Operator Health	+2	-2	-1	-1
Environmental effect	+2	-2	+1	+1
Cost of coolant	+2	-2	+1	+1
Recycling and disposal	+2	-2	+2	+2
Part cleaning	-2	-1	+1	+1
Surface quality	-2	+1	+1	+2
Total score	4	-8	5	6

with dry, flood, and MQL-MO cutting conditions. The reduction in tool wear can be attributed to the reduction in friction coefficient provided by the CO molecules at the workpiece-tool-chip interfaces.

- A smooth machined surface was identified under MQL-CO cutting with an improvement of 48%, 31%, and 19% in correlation with dry, flood, and MQL-MO cutting conditions. This improvement was facilitated by the formation of thick lubricating film on the workpiece surfaces by the CO molecules which led to reduce the friction between the interacting surfaces.
- The temperature at the cutting region was decreased by 56%, 37%, and 21% with MQL-CO cutting in comparison with dry, flood, and MQL-MO cutting conditions. This reduction in cutting temperature can be ascribed to the effective heat dissipation of CO molecules along with pressurized air with the MQL technique.
- The application of MQL-CO resulted in lesser tool vibration during the metal-cutting operation compared

to other selected cutting conditions. The reduction in friction between the interacting surfaces and effective removal of chips from the cutting region resulted in lesser cutting forces and ultimately lesser tool vibration levels.

- Chip morphology obtained under the MQL-CO condition showed small serrations and fewer scratches than that of other selected cutting conditions.
- The sustainability assessment showed that the MQL-CO appears to be a feasible alternative to conventional mineral-based cutting fluids with less impact on human health and environmental ecology.

## 6 Future scope of work

This study presented the aptness of vegetable oil with MQL to improve the machining performance of AISI-1040 steel. In this domain, the effect of various sizes and different concentrations of nanoparticles on the machinability of hardened steel can be considered in the future. Also, the other assessment models such as life cycle assessment (LCA), economic analysis, total cycle time, and productivity can be explored in the future to investigate the effects of nanofluids on the environmental and economic aspects.

**Author contributions** Saurabh Tiwari: conceptualization, methodology, investigation, writing-original draft, data curation.

Amarnath M: conceptualization, supervision, review and editing.

**Data availability** The raw/processed data required to reproduce these findings cannot be shared at this time as the data also forms part of an ongoing study.

## Declarations

**Ethical approval** Not applicable

**Competing interest** The authors declare no competing interests.

## References

- Yan P, Rong Y, Wang G (2015) The effect of cutting fluids applied in metal cutting process. <https://doi.org/10.1177/0954405415590993>
- Gaurav G, Sharma A, Dangayach GS, Meena ML (2020) Assessment of jojoba as a pure and nano-fluid base oil in minimum quantity lubrication (MQL) hard-turning of Ti-6Al-4V: A step towards sustainable machining. *J Clean Prod* 272:122553. <https://doi.org/10.1016/j.jclepro.2020.122553>
- Yıldırım ÇV, Kivak T, Sarıkaya M, Şirin Ş (2020) Evaluation of tool wear, surface roughness/topography and chip morphology when machining of Ni-based alloy 625 under MQL, cryogenic cooling and CryoMQL. *J Mater Res Technol* 9(2):2079–2092



4. Paul S, Dhar NR, Chattopadhyay AB (2001) Beneficial effects of cryogenic cooling over dry and wet machining on tool wear and surface finish in turning AISI 1060 steel. *J Mater Process Technol* 116(1):44–48. [https://doi.org/10.1016/S0924-0136\(01\)00839-1](https://doi.org/10.1016/S0924-0136(01)00839-1)
5. Rahim EA, Dorairaju H (2018) Evaluation of mist flow characteristic and performance in minimum quantity lubrication (MQL) machining. *Meas: J Int Meas Confed* 123:213–225. <https://doi.org/10.1016/j.measurement.2018.03.015>
6. Ruggiero A, Amato RD, Merola M, Vala P (2017) Tribological characterization of vegetal lubricants : comparative experimental investigation on *Jatropha curcas L . oil* , Rapeseed Methyl Ester oil , Hydrotreated Rapeseed oil. *Tribol Int* 109:529–540. <https://doi.org/10.1016/j.triboint.2017.01.030>
7. Sen B, Mia M, Krolczyk GM, Mandal UK, Mondal SP (2019) Eco-Friendly cutting fluids in minimum quantity lubrication assisted machining: a review on the perception of sustainable manufacturing, no. 0123456789. *Korean Society for Precision Engineering*. <https://doi.org/10.1007/s40684-019-00158-6>
8. Deiai I, Raza SW, Pervaiz S (2014) Analysis of lubrication strategies for sustainable machining during turning of titanium ti-6al-4v alloy. *Procedia CIRP* 17:766–771. <https://doi.org/10.1016/j.procir.2014.01.112>
9. Bahari A, Lewis R, Slatter T (2018) Friction and wear phenomena of vegetable oil-based lubricants with additives at severe sliding wear conditions. *Tribol Trans* 61(2):207–219. <https://doi.org/10.1080/10402004.2017.1290858>
10. Ojolo SJ, Amuda MOH, Ogunmola OY, Ononiwu CU (2008) Experimental determination of the effect of some straight biological oils on cutting force during cylindrical turning. *Matéria (Rio de Janeiro)* 13(4):650–663. <https://doi.org/10.1590/s1517-70762008000400011>
11. Gupta MK, Boy M, Korkmaz ME, Yaşar N, Günay M, Krolczyk GM (2022) Measurement and analysis of machining induced tribological characteristics in dual jet minimum quantity lubrication assisted turning of duplex stainless steel. *Measurement* 187:110353
12. Ekinović S, Begović E, Lušija A (2014) MQL machining—oil on water droplet system. *IBU J Sci Technol* 2014:15. <https://eprints.ibu.edu.ba/items/show/518>
13. Kanagaraju T et al (2022) Experimental analysis on drilling of super duplex stainless steel 2507 (SDSS 2507) using cryogenic LCO2 and MQL process. *Biomass Convers Biorefin* 2507(Sdss 2507). <https://doi.org/10.1007/s13399-022-02536-8>
14. Sen B, Kumar M, Mia M, Kumar U (2020) Tribology International Wear behaviour of TiAlN coated solid carbide end-mill under alumina enriched minimum quantity palm oil-based lubricating condition. *Tribol Int* 148:106310. <https://doi.org/10.1016/j.triboint.2020.106310>
15. Revuru RS, Zhang JZ, Posinasetti NR (2020) Comparative performance studies of turning 4140 steel with TiC/TiCN/TiN-coated carbideinserts using MQL, flooding with vegetable cutting fluids, and dry machining. *Int J Adv Manuf Technol* 108:381–391. <https://doi.org/10.1007/s00170-020-05378-8>
16. Özbek O, Saruhan H (2020) The effect of vibration and cutting zone temperature on surface roughness and tool wear in eco-friendly MQL turning of AISI D2. *J Mater Res Technol* 9(3):2762–2772. <https://doi.org/10.1016/j.jmrt.2020.01.010>
17. Vamsi Krishna P, Srikant RR, Nageswara Rao D (2010) Experimental investigation on the performance of nanoboric acid suspensions in SAE-40 and coconut oil during turning of AISI 1040 steel. *Int J Mach Tools Manuf* 50(10):911–916. <https://doi.org/10.1016/j.jmachtools.2010.06.001>
18. Wang X et al (2020) Vegetable oil-based nanofluid minimum quantity lubrication turning: Academic review and perspectives. *J Manuf Process* 59:76–97. <https://doi.org/10.1016/j.jmapro.2020.09.044>
19. Liu D, Li C, Dong L, Qin A, Zhang Y, Yang M et al (2022) Kinematics and improved surface roughness model in milling. *Int J Adv Manuf Technol*. <https://doi.org/10.1007/s00170-022-10729-8>
20. Wang X et al (2022) Tribology of enhanced turning using biolubricants: a comparative assessment. *Tribol Int* 174:107766. <https://doi.org/10.1016/j.triboint.2022.107766>
21. Paramasivam B (2020) Investigation on the effects of damping over the temperature distribution on internal turning bar using infrared fusion thermal imager analysis via SmartView software. *Meas: J Int Meas Confed* 162:107938. <https://doi.org/10.1016/j.measurement.2020.107938>
22. Arrazola P-J, Aristimuno P, Soler D, Childs T (2015) Metal cutting experiments and modelling for improved determination of chip/tool contact temperature by infrared thermography. *CIRP Ann* 64(1):57–60
23. Prasad BS, Prabha KA, Kumar PVSG (2017) Condition monitoring of turning process using infrared thermography technique – an experimental approach. *Infrared Phys Technol* 81:137–147. <https://doi.org/10.1016/j.infrared.2016.12.023>
24. Şirin Ş, Sarıkaya M, Yıldırım ÇV, Kivak T (2020) Machinability performance of nickel alloy X-750 with SiAlON ceramic cutting tool under dry, MQL and hBN mixed nanofluid-MQL. *Tribol Int* 153:2021. <https://doi.org/10.1016/j.triboint.2020.106673>
25. Gupta MK et al (2021) Experimental characterisation of the performance of hybrid cryo-lubrication assisted turning of Ti–6Al–4V alloy. *Tribol Int* 153:106582. <https://doi.org/10.1016/j.triboint.2020.106582>
26. Orhan S, Er AO, Camuşcu N, Aslan E (2007) Tool wear evaluation by vibration analysis during end milling of AISI D3 cold work tool steel with 35 HRC hardness. *NDT E Int* 40:121–126. <https://doi.org/10.1016/j.ndteint.2006.09.006>
27. Rmili W, Ouahabi A, Serra R, Leroy R (2016) An automatic system based on vibratory analysis for cutting tool wear monitoring. *Meas: J Int Meas Confed* 77:117–123. <https://doi.org/10.1016/j.measurement.2015.09.010>
28. Ragai I, Abdalla AS, Abdeltawab H, Qian F, Ma J (2022) Toward smart manufacturing: analysis and classification of cutting parameters and energy consumption patterns in turning processes. *J Manuf Syst* xxxx. <https://doi.org/10.1016/j.jmsy.2022.04.016>
29. Sivalingam V, Zhao Y, Thulasiram R, Sun J, Kai G, Nagamalai T (2021) Machining Behaviour, surface integrity and tool wear analysis in environment friendly turning of Inconel 718 alloy. *Meas: J Int Meas Confed* 174:109028. <https://doi.org/10.1016/j.measurement.2021.109028>
30. Fernandes P, Prabhu KN (2008) Comparative study of heat transfer and wetting behaviour of conventional and bioquenchant for industrial heat treatment. *Int J Heat Mass Transf* 51(3–4):526–538. <https://doi.org/10.1016/j.ijheatmasstransfer.2007.05.018>
31. Najiha MS, Rahman MM, Yusoff AR (2015) Flank Wear characterization in aluminum alloy (6061 t6) with nanofluid minimum quantity lubrication environment using an uncoated carbide tool. *J Manuf Sci E T ASME* 137(6):1–27. <https://doi.org/10.1115/1.4030060>
32. Aslan A (2020) Optimization and analysis of process parameters for flank wear, cutting forces and vibration in turning of AISI 5140: a comprehensive study. *Meas: J Int Meas Confed* 163:107959. <https://doi.org/10.1016/j.measurement.2020.107959>
33. Ajay Vardhaman BS, Amarnath M, Jhodkar D, Ramkumar J, Chelladurai H, Roy MK (2018) Influence of coconut oil on tribological behavior of carbide cutting tool insert during turning operation. *J Braz Soc Mech Sci Eng* 40(9):1–23. <https://doi.org/10.1007/s40430-018-1379-y>
34. Zhang Y et al (2022) Nano-enhanced biolubricant in sustainable manufacturing: From processability to mechanisms. *Friction* 10(6):803–841. <https://doi.org/10.1007/s40544-021-0536-y>



35. Xu W, Li C, Zhang Y, Ali HM, Sharma S, Li R et al (2022) Electrostatic atomization minimum quantity lubrication machining: from mechanism to application. *Int J Extrem Manuf* 4:042003. <https://doi.org/10.1088/2631-7990/ac9652>
36. Jayadas NH, Nair KP (2006) Coconut oil as base oil for industrial lubricants-evaluation and modification of thermal, oxidative and low temperature properties. *Tribol Int* 39(9):873–878. <https://doi.org/10.1016/j.triboint.2005.06.006>
37. Koshy CP, Rajendrakumar PK, Thottackkad MV (2015) Evaluation of the tribological and thermo-physical properties of coconut oil added with MoS<sub>2</sub> nanoparticles at elevated temperatures. *Wear* 330:288–308
38. Sujith SV, Solanki AK, Mulik RS (2019) Experimental evaluation on rheological behavior of Al<sub>2</sub>O<sub>3</sub>-pure coconut oil nanofluids. *J Mol Liq* 286:110905
39. Saez-de-Buruaga M, Soler D, Aristimuño PX, Esnaola JA, Arrazola PJ (2018) Determining tool/chip temperatures from thermography measurements in metal cutting. *Appl Therm Eng* 145:305–314. <https://doi.org/10.1016/j.applthermaleng.2018.09.051>
40. Soler D, Aristimuño PX, Saez-de-Buruaga M, Garay A, Arrazola PJ (2018) New calibration method to measure rake face temperature of the tool during dry orthogonal cutting using thermography. *Appl Therm Eng* 137:74–82. <https://doi.org/10.1016/j.appltherma.2018.03.056>
41. Prabhu KN, Fernandes P, Kumar G (2009) Effect of substrate surface roughness on wetting behaviour of vegetable oils. *Mater Des* 30(2):297–305. <https://doi.org/10.1016/j.matdes.2008.04.067>
42. Derani MN, Ratnam MM (2021) The use of tool flank wear and average roughness in assessing effectiveness of vegetable oils as cutting fluids during turning—a critical review. *Int J Adv Manuf Technol* 112(7–8):1841–1871. <https://doi.org/10.1007/s00170-020-06490-5>
43. Agrawal C, Wadhwa J, Pitroda A, Pruncu CI, Sarikaya M, Khanna N (2021) Comprehensive analysis of tool wear, tool life, surface roughness, costing and carbon emissions in turning Ti–6Al–4V titanium alloy: Cryogenic versus wet machining. *Tribol Int* 153:106597. <https://doi.org/10.1016/j.triboint.2020.106597>
44. Zeng Q, Qin Y, Chang W, Luo X (2018) Correlating and evaluating the functionality-related properties with surface texture parameters and specific characteristics of machined components. *Int J Mech Sci* 149:62–72. <https://doi.org/10.1016/j.ijmecsci.2018.09.044>
45. Sujith SV, Mulik RS (2022) Surface Integrity and flank wear response under pure coconut oil-Al<sub>2</sub>O<sub>3</sub> nano minimum quantity lubrication turning of Al-7079/7 wt%-TiC in situ metal matrix composites. *J Tribol* 144(5):1–15. <https://doi.org/10.1115/1.4051863>
46. Leksycki K, Królczyk JB (2020) Comparative assessment of the surface topography for different optical profilometry techniques after dry turning of Ti6Al4V titanium alloy. *Meas: J Int Meas Confed* 169. <https://doi.org/10.1016/j.measurement.2020.108378>
47. Gök F, Orak S, Sofuoğlu MA (2020) The effect of cutting tool material on chatter vibrations and statistical optimization in turning operations. *Soft Comput* 24(22):17319–17331. <https://doi.org/10.1007/s00500-020-05022-3>
48. Siddhpura M, Paurobally R (2012) A review of chatter vibration research in turning. *Int J Mach Tools Manuf* 61:27–47. <https://doi.org/10.1016/j.ijmachtools.2012.05.007>
49. Prasad BS, Sarcar MMM, Ben BS (2010) Development of a system for monitoring tool condition using acousto-optic emission signal in face turning-an experimental approach. *Int J Adv Manuf Technol* 51(1–4):57–67. <https://doi.org/10.1007/s00170-010-2607-5>
50. Airao J, Nirala CK, Bertolini R, Krolczyk GM, Khanna N (2022) Sustainable cooling strategies to reduce tool wear, power consumption and surface roughness during ultrasonic assisted turning of Ti-6Al-4V. *Tribol Int* 169:107494. <https://doi.org/10.1016/j.triboint.2022.107494>
51. Dash L, Padhan S, Das SR (2020) Experimental investigations on surface integrity and chip morphology in hard turning of AISI D3 steel under sustainable nanofluid-based minimum quantity lubrication. *J Braz Soc Mech Sci Eng* 42(10):500. <https://doi.org/10.1007/s40430-020-02594-x>
52. Mia M, Gupta MK, Singh G, Królczyk G, Pimenov DY (2018) An approach to cleaner production for machining hardened steel using different cooling-lubrication conditions. *J Clean Prod* 187:1069–1081. <https://doi.org/10.1016/j.jclepro.2018.03.279>
53. Ross NS, Mia M, Anwar S, Manimaran G, Saleh M, Ahmad S (2021) A hybrid approach of cooling lubrication for sustainable and optimized machining of Ni-based industrial alloy. *J Clean Prod* 321:128987
54. Padhan S, Das A, Santoshwar A, Dharmendrabhai TR, Das SR (2021) Sustainability assessment and machinability investigation of austenitic stainless steel in finish turning with advanced ultra-hard SiAlON ceramic tool under different cutting environments. *Silicon* 13:119–147

**Publisher's note** Springer Nature remains neutral with regard to jurisdictional claims in published maps and institutional affiliations.

Springer Nature or its licensor (e.g. a society or other partner) holds exclusive rights to this article under a publishing agreement with the author(s) or other rightsholder(s); author self-archiving of the accepted manuscript version of this article is solely governed by the terms of such publishing agreement and applicable law.